Inorganic Chemistry



pubs.acs.org/IC
Article

# Mixed Phenanthroline–Bipyridine Europium and Ytterbium Cryptates—Bright Luminophores with Small Radiative Lifetimes

Tobias Haas, Timo Neumann, Nicholas Jobbitt, Xiaoyu Yang, Hartmut Schubert, David Hunger, and Michael Seitz*

Cite This: https://doi.org/10.1021/acs.inorgchem.5c05828
Read Online



**ABSTRACT:** New phenanthroline-based tris(biaryl) europium(III) and ytterbium(III) cryptates with great luminescence efficiencies in solution are reported. 1,10-Phenantroline, in combination with 2,2′-bipyridine-*N*,*N*′-dioxide, delivers cryptates with high rigidity, efficient lanthanoid(III) sensitization ($\eta_{sens}$) and small radiative lifetimes $\tau_{rad}$ for Eu and Yb. The powerful synergy of both bidentate chelating units results in excellent absolute quantum yields of up to 20% for the europium complexes in aqueous solution, which indicates an impressive improvement compared to other well-known tris(bipyridyl)-based Eu(III) cryptates.

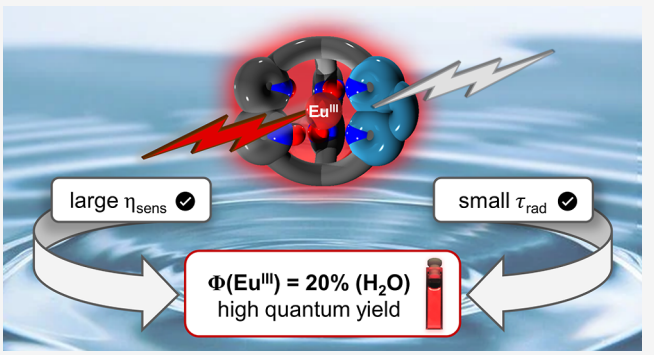




## INTRODUCTION

Photoluminescence in molecular lanthanoid complexes has found a wide array of fascinating applications due to their unique properties over the last decades.[1] While most of the processes affecting lanthanoid luminescence (such as energy transfer from the ligand to the metal or intramolecular quenching of excited states) have been investigated and optimized thoroughly, the radiative luminescence lifetime $\tau_{rad}$ is still not completely understood.[2] In contrast to the measured (observed) luminescence lifetime $\tau_{obs}$, the radiative lifetime $\tau_{rad}$ of an excited state is the hypothetical luminescence lifetime in the absence of any other nonradiative deactivating processes. Little attention has been paid to this key parameter over the last decades, despite its important role in determining the absolute quantum yield $Q_{Ln}^{L}$ as can be seen in eq 1

$$Q_{Ln}^{L} = \eta_{sens} \cdot Q_{Ln}^{Ln} = \eta_{sens} \cdot \frac{\tau_{obs}}{\tau_{rad}} \quad (1)$$

The absolute quantum yield is determined by the sensitization efficiency $\eta_{sens}$ (including intersystem crossing and energy transfer from the ligand to the lanthanoid) and by the intrinsic quantum yield $Q_{Ln}^{Ln}$. The intrinsic quantum yield is equal to the ratio of the observed radiative rate constant $k_r$ ($=1/\tau_{rad}$) and the nonradiative deactivation rate constant $k_{nr}$ according to eq 2

$$Q_{Ln}^{Ln} = \frac{k_r}{k_r + k_{nr}} \quad (2)$$

eqs 1 and 2 make clear that increasing the overall quantum yield $Q_{Ln}^{L}$ is dependent on the simultaneous optimization of a whole set of parameters ($\eta_{sens}$, $k_r = 1/\tau_{rad}$, $k_{nr}$). Nevertheless, when hypothetically leaving all factors other than $\tau_{rad}$ constant, decreasing the radiative lifetime makes the emission more competitive compared to nonradiative deactivation processes which leads to higher emission efficiencies. It should be pointed out that the total light intensity that can be detected does not depend solely on the absolute quantum yield $Q_{Ln}^{L}$ but instead should be evaluated using the brightness $B$ ($B = Q_{Ln}^{L} \cdot \varepsilon$), which also takes into account the molar extinction coefficient $\varepsilon$ at the excitation wavelength. In addition, the question if a particular application benefits from short (e.g., most OLED applications) or long (e.g., time-gated luminescence bioassays) observable luminescence lifetimes $\tau_{obs}$ is also connected to whether short or long intrinsic lifetimes $\tau_{rad}$ are advantageous.

Since the valence f-orbitals in trivalent lanthanoids are shielded from covalent interactions with the surrounding by filled 5s/5p-orbitals, f–f-transitions are relatively strictly Laporte-forbidden. In contrast to e.g. transition metal complexes, here this selection rule cannot easily be relaxed by admixture of states/vibrations of opposite parity. Therefore, influencing $\tau_{rad}$ in $Ln^{3+}$ ions is not straightforward and our knowledge in this area is quite fragmentary.[2] There are still only very few examples in the literature where changes in

Received: December 13, 2025
Revised: February 4, 2026
Accepted: February 6, 2026

radiative lifetimes can be assigned unambiguously to modifications of the coordination sphere of the lanthanoid ion instead of depending on a completely different donor set.

Our interest in this subject was initiated by investigations of Bünzli et al. that the bidentate ligand 2,2′-bipyridine-*N*,*N*′-dioxide is able to decrease the radiative lifetime in europium(III) β-diketonate complexes substantially.[3] Related work by us later confirmed an analogous effect for tris(bipyridine)-based cryptates of Yb, Eu, and Nd (Figure 1).[4,5]

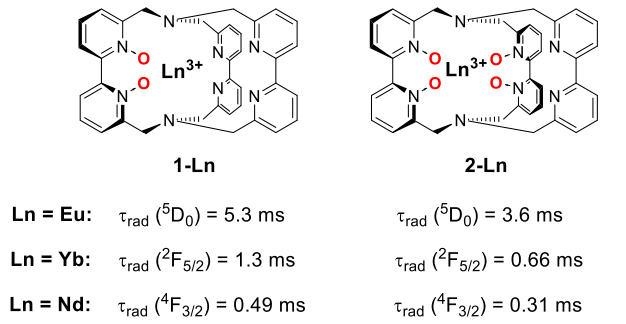


**Figure 1.** Tris(bipyridine)-based lanthanoid cryptates **1-Ln** and **2-Ln** with different contents of pyridine-*N*-oxide moieties and their influence on $\tau_{rad}$.[4,5]

In the studies on europium[5] and ytterbium[4] we showed that more pyridine-*N*-oxide binding motifs in cryptates are responsible for an increased rate of emission. Concomitantly, however, the 2,2′-bipyridine-*N*,*N*′-dioxide units unfortunately had a negative influence on sensitization efficiencies $\eta_{sens}$, which inevitably led to reduced absolute quantum yields, especially in the case for europium.[5] This unwanted effect presumably resulted from the introduction of low-lying CT states through higher *N*-oxide contents, which seems plausible for europium and ytterbium, both of them having accessible divalent oxidation states.[6] In an effort to alleviate this problem, we turned our attention to other reports in the literature that 1,10-phenanthroline has a similar impact compared to pyridine-*N*-oxides for reducing radiative lifetimes in luminescent europium complexes. For example, $\tau_{rad}$ of the europium(III) β-diketonate complex **4-Eu** using 1,10-phenanthroline as ancillary ligand is 23% smaller compared to its 2,2′-bipyridine analogue **3-Eu** (see Figure 2).[7] In a second example, it was shown in the literature that 1,10-phenanthroline is responsible for an efficient energy transfer in europium(III) nitrate complex $[Eu(phen)_2(NO_3)_3]$ ($\eta_{sens}$ = 72%).[8] Based on the previous literature precedence, 1,10-phenanthroline seemed to us in this context to be an attractive photosensitizer in addition to its generally beneficial properties of also being much more rigid than 2,2′-bipyridine.[9]

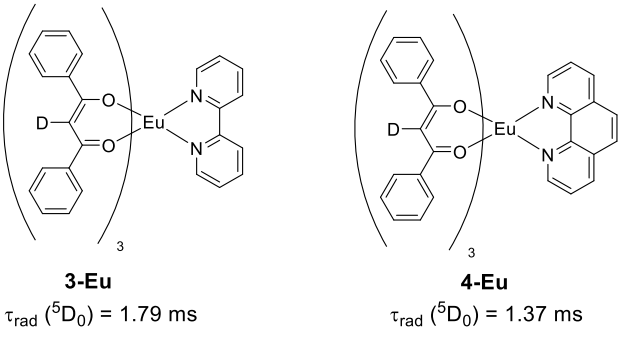


**Figure 2.** Europium β-diketonate complexes **3-Eu** and **4-Eu** using 2,2′-bipyridine and 1,10-phenanthroline as ancillary ligands, respectively.[6]

Here, we expand our previous study for europium and ytterbium tris(bipyridine) cryptates[4,5] by combining 2,2′-bipyridine-*N*,*N*′-dioxide motifs with 1,10-phenanthroline in cryptate scaffolds in order to achieve further insights into how the radiative lifetime $\tau_{rad}$ can be utilized in a systematic manner to modulate the luminescence in these lanthanoid complexes. We also exclusively focus on the pure photophysics in order to enhance the overall quantum yield $Q^L_{Ln}$ without taking into account practical considerations such as brightness or application-specific requirements.

For this purpose, we designed the two novel cryptates **5-Ln** and **6-Ln** (Figure 3) which are very similar to the tris(2,2′-bipyridine)-based cryptates **1-Ln** and **2-Ln** (Figure 1). The former share as many features as possible and only differ in the number of (a) *N*-oxide donor moieties and (b) phenanthroline motifs. Moreover, all mentioned cryptates (**1-Ln**, **2-Ln**, **5-Ln**, **6-Ln**) exhibit $C_2$-symmetric structures in solution. The similarities among all tris(bipyridine) cryptates provide a perfect setup for the interpretation of the changes in radiative lifetimes $\tau_{rad}$ and sensitization efficiencies $\eta_{sens}$. For the Yb cryptates, where strong multiphonon quenching of the metal-centered, excited states by ligand C−H oscillators can be expected,[10] we also prepared the partially deuterated cryptate **[D8]-6-Yb** (Figure 3), in order to also study the effect that deuteration has on the improvement of luminescence efficiencies.

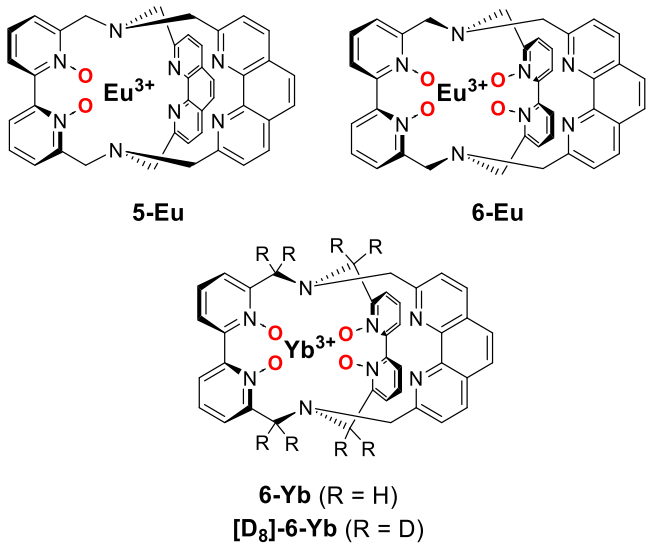


**Figure 3.** New lanthanoid cryptates **5-Eu**, **6-Eu**, **6-Yb**, and **[D8]-6-Yb** with different contents of (partially deuterated) pyridine-*N*-oxide moieties and 1,10-phenanthroline units used in this study.

## RESULTS AND DISCUSSION

### Cryptate Synthesis

The usual approach for synthesizing macrobicyclic cryptates is the reaction of diamines and dibromides in appropriate ratios (Scheme 1). For the synthetic realization of the desired cryptands **5** and **6**, different building blocks are essential. Benzylic phenanthroline diamine **7** was obtained as trihydro-


https://doi.org/10.1021/acs.inorgchem.5c05828
Inorg. Chem. XXXX, XXX, XXX−XXX

**Scheme 1. Synthesis of the Lanthanoid Cryptates 5-Eu, 6-Eu, 6-Yb, and [$D_8$]-6-Yb**

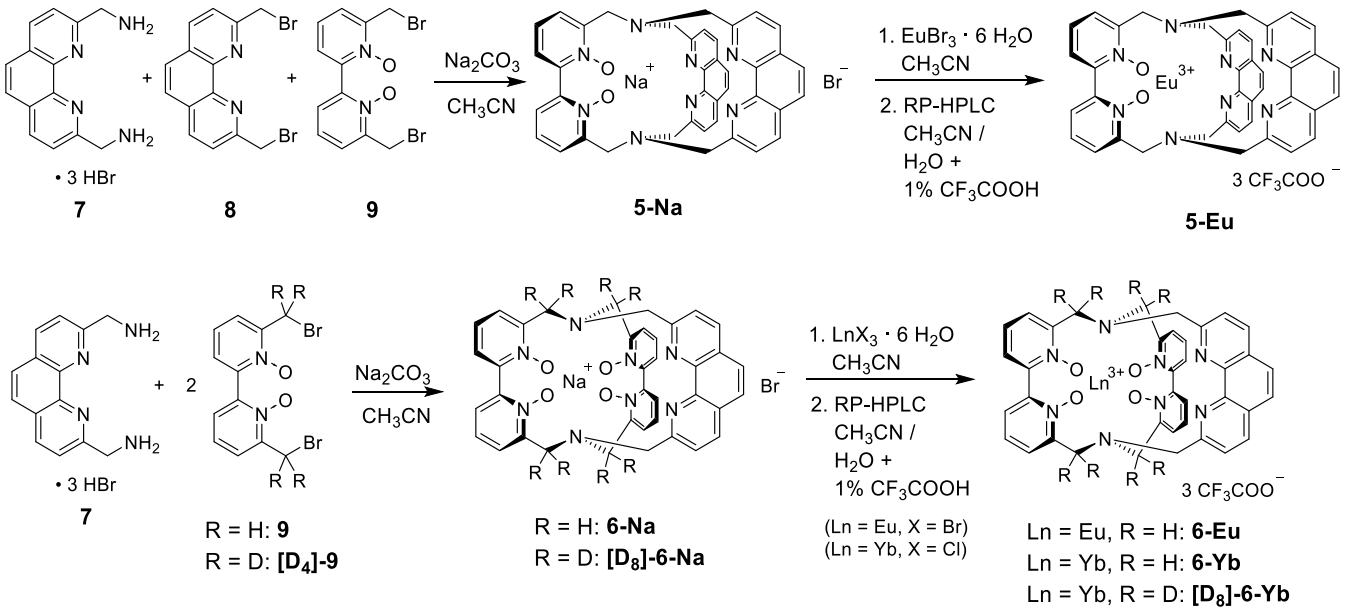


bromide salt by the Delépine reaction of dibromide **8** with hexamethylenetetramine followed by acid hydrolysis of the resulting quaternary ammonium salt.[11] The known dibromide precursors **8**[12] and **9**[13]/[$D_4$]-**9**[14] were synthesized according to known literature procedures.

The sodium cryptate **5-Na** which features two 1,10-phenanthroline motifs, was obtained by reacting the building blocks **7**, **8** and **9** in an equimolar ratio with sodium carbonate in acetonitrile (Scheme 1). This is, to the best of our knowledge, the first reported one-step cryptate synthesis using three different precursors. Unsurprisingly, two other cryptate species, **6-Na** and the sodium cryptate with the known cryptand [phen.phen.phen][15] occurred as byproducts of this one-step macrobicycle formation which could be separated by column chromatography. Nevertheless, the obtained isolated yield for **5-Na** of 26% (see the Experimental Section) is quite respectable for such a complicated reaction and this approach proved the most economical synthetic route to **5-Na**. Macrocyclization using precursors **7** and either **9** or the partially deuterated isotopologue [$D_4$]-**9** in appropriate ratios (1:2) gave sodium cryptates **6-Na** and [$D_8$]-**6-Na**, both containing two 2,2′-bipyridine-*N*,*N*′-dioxide- and one 1,10-phenanthroline unit (Scheme 1).

It is important to purify the sodium complexes **6-Na** via column chromatography on aluminum oxide to avoid $Ca^{2+}$ contamination (present in commerical silica).[16] All sodium cryptates **5-Na** and **6-Na**/[$D_8$]-**6-Na** could be converted to the corresponding lanthanoid species by metal exchange with europium tribromide hexahydrate or ytterbium trichloride hexahydrate in boiling acetonitrile. Reversed-phase HPLC purification (see the Supporting Information for more details) of the obtained crude mixtures yielded **5-Eu**, **6-Ln** (Ln = Eu, Yb), and [$D_8$]-**6-Yb** as trifluoroacetate salts.

It should be noted here that all new lanthanoid cryptates exhibit (in alignment with the well-known **1-Eu** and **2-Eu**[5]) excellent (kinetic) stability under the relatively harsh HPLC conditions ($H_2O$ + 1% $CF_3COOH$/$CH_3CN$). The lanthanoid cryptates are highly soluble in polar, protic solvents (e.g., $H_2O$, $CH_3OH$), slightly soluble in polar, aprotic solvents (e.g., $CH_3CN$) and almost insoluble in nonpolar solvents (e.g., $CH_2Cl_2$). In addition to the europium and ytterbium complexes, the diamagnetic lutetium analogues **5-Lu** and **6-Lu** were obtained as diamagnetic and f−f photoinactive control compounds by the same synthetic procedures (see the Experimental Section).

## Structural Properties

Single crystals suitable for X-ray analysis were obtained by layering a methanolic solution of sodium cryptate **6-Na** with diethyl ether. The cryptate structure shows an eight-coordinate sodium center in an overall $C_2$-symmetric complex (Figure 4). The sodium cation is completely shielded by the cryptand and does not bind to any additional, external ligand. As expected, the molecular structure exhibits the twisted 2,2′-bipyridine-

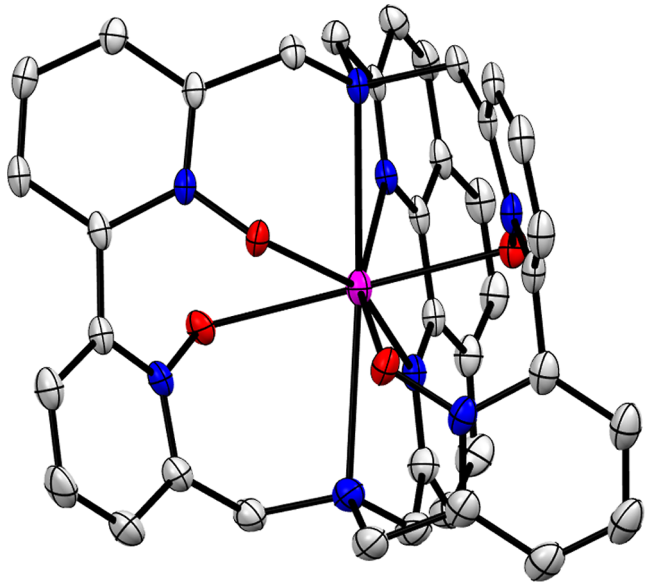

**Figure 4.** Thermal ellipsoid plot (Ortep 3 for Windows,[17] 50% probability level) for the cation of **6-Na** (CCDC No. 2184715). The hydrogen atoms, the free bromide anion and the isolated water and methanol molecules are omitted for clarity.


https://doi.org/10.1021/acs.inorgchem.5c05828
Inorg. Chem. XXXX, XXX, XXX−XXX

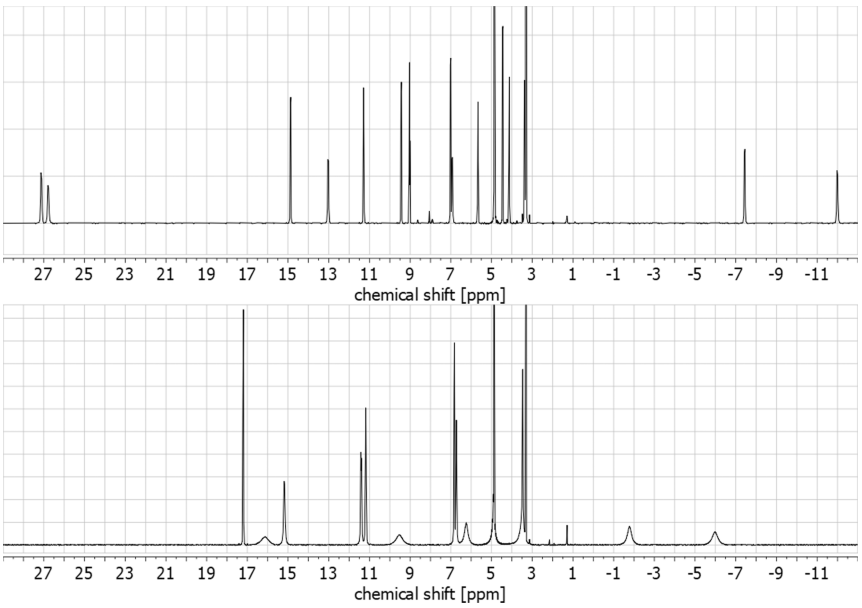


**Figure 5.** $^{1}$H NMR spectra ($CD_3OD$, 400 MHz) of **5-Eu** (top) and **6-Eu** (bottom).

*N,N′*-dioxide motifs and the rigidly planar 1,10-phenanthroline in the cryptate scaffold.

The binding properties of the phenanthroline are unremarkable and resemble the ones found in the crystal structure of the sodium cryptate with the known cryptand [phen.phen.phen].[15b] Unfortunately, we were not successful in obtaining single crystals suitable for X-ray analysis of **5-Na** and the lanthanoid cryptates.

NMR investigation of the cryptates in solution was possible for all cryptates. $^{1}$H NMR spectroscopy clearly exhibited one $C_2$-symmetric cryptate species in $CD_3OD$ in each case (e.g., see the NMR spectra of **5-Eu** and **6-Eu** in Figure 5). $^{1}$H NMR spectra of sodium cryptates **5-Na** and **6-Na** showed three well-defined AB systems for the benzylic methylene protons which are consistent with other *N*-oxide containing tris(biaryl) cryptates with atropisomeric stereogenic elements (see Figures S2 and S3 in the Supporting Information for more details).

## Photophysical Properties

**Ligand-Centered Photophysics.** To achieve maximum similarity between the present and our previous studies, the europium and ytterbium cryptates were mainly investigated in $D_2O$[5] and in $CD_3OD$,[4] respectively. The UV/vis absorption spectra of **5-Eu** and **6-Ln** (see Figures S15 and S16 in the Supporting Information) show characteristic bands in the spectral region from 280 to ca. 360 nm, even though the bands are slightly different dependent on the phenanthroline content of the current cryptate. The spectrum of **5-Eu**, featuring two phenanthroline motifs, extends a little bit further into the long-wavelength range. To get further insight into the energy transfer from the cryptands to the lanthanoids, we investigated the corresponding lutetium cryptates **5-Lu** and **6-Lu** by determining their zero-phonon $T_1 \rightarrow S_0$ transition energy $E(T_1)$ by low-temperature (77 K) emission spectra (see Figure S17 in the Supporting Information). The lack of vibronic structures of the phosphorescence bands prevents the exact determination of $E(T_1)$. A rough estimate, however, of the possible range for **5-Lu** is $E(T_1) \approx 20{,}200-21{,}000$ cm$^{-1}$, which is in the range of tris(bipyridine) cryptand **1** ($E(T_1) \approx 20{,}400$ cm$^{-1}$).[4] Tetra *N*-oxide cryptate **6-Lu** exhibits a significantly higher triplet level, $E(T_1) \approx 23{,}500-25{,}000$ cm$^{-1}$ (400−425 nm), which is in agreement with measurements of tris(bipyridine) cryptates in our previous study where a higher *N*-oxide content afforded a higher triplet energy (cryptand **2** ($E(T_1) \approx 22{,}600$ cm$^{-1}$).[4] The measured triplet levels in **5-Lu** and **6-Lu** are both well above the emitting $^{5}D_0$ state of $Eu^{3+}$ ($^{5}D_0 \approx 17{,}300$ cm$^{-1}$),[18] and the excited $^{2}F_{7/2}$ level of $Yb^{3+}$ ($^{2}F_{7/2} \approx 10{,}300$ cm$^{-1}$),[19] thus avoiding any thermal energy back transfer from the lanthanoid center to the ligand-centered triplet state.

**Europium.** Steady-state emission of cryptates **5-Eu** and **6-Eu** in $D_2O$ show strong luminescence with the characteristic europium bands originating from the excited $^{5}D_0$ state (Figure 6). Both spectra exhibit only one single peak for each $^{5}D_0 \rightarrow {}^{7}F_0$ transition, suggesting the presence of only one emitting species in solution in each case. Along the lines of the tris(bipyridine) analogues,[5] an increase in *N*-oxide content is accompanied by an increase in the $^{5}D_0 \rightarrow {}^{7}F_0$ energies (see Table 1 and Figure 6). Due to their high sensitivity to the coordination environment, europium spectra contain a lot of

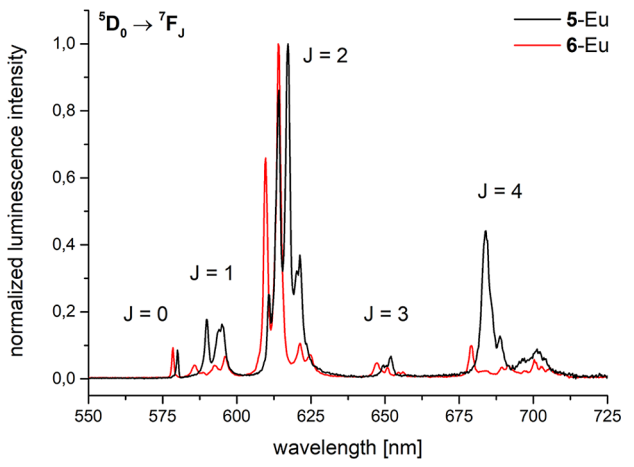


**Figure 6.** Steady-state emission spectra ($D_2O$, $c \approx 10$ $\mu$M) for **5-Eu** (black, $\lambda_{exc} = 300$ nm) and **6-Eu** (red, $\lambda_{exc} = 318$ nm).



https://doi.org/10.1021/acs.inorgchem.5c05828
Inorg. Chem. XXXX, XXX, XXX−XXX

Table 1. Luminescence Data for the Europium Cryptates 5-Eu and 6-Eu in $D_2O$ ($H_2O$)

| compd. | $\tilde{\nu}(^5D_0 \rightarrow {}^7F_0)$ [$cm^{-1}$] | $\tau_{obs(D)}$ ($\tau_{obs(H)}$) [ms] | $q$[b] | $\tau_{rad}$ [ms] | $Q_{Eu}^{Eu} = \frac{\tau_D}{\tau_{rad}}$ [%] | $Q_{Eu}^{L}$ [%] | $\eta_{sens}$ [%] |
|---|---|---|---|---|---|---|---|
| **1-Eu**[5] | 17283 | 1.61 (0.54) | 1.2 | 5.3 | 30 | 7.6 | 25 |
| **2-Eu**[5] | 17301 | 1.00 (0.43) | 1.3 | 3.6 | 28 | 4.2 | 15 |
| **5-Eu** | 17241 | 1.33 (0.71)[a] | 0.5 | 2.9[c] | 46[d] | 36 (20)[e] | 78[f] |
| **6-Eu** | 17301 | 1.00 (0.57)[a] | 0.6 | 2.0[c] | 50[d] | 42 (20)[e] | 83[f] |

[a]Luminescence lifetimes: $\lambda_{exc}$ = 300 nm, $\lambda_{em}$ = 615 nm ($^5D_0 \rightarrow {}^7F_2$), estimated uncertainty ±10%. [b]Number of inner-sphere water molecules, see ref 23. [c]Radiative lifetime calculated using eq 3, estimated uncertainty ±20%. [d]Intrinsic quantum yield, estimated uncertainty ±30%. [e]Absolute quantum yield, measured using quinine sulfate (in 0.1 M $H_2SO_4$) as standard (ref 25), values in $H_2O$ in parentheses, estimated uncertainty ±10%. [f]Sensitization efficiency (see eq 1).

information on the molecular structure in solution.[20] The obtained bands (Figure 6) validate the observed $C_2$-symmetry by $^1H$ NMR spectroscopy in solution (vide supra). The splitting patterns of the emissive transitions indicate a coordination environment with low symmetry around the trivalent europium cation.[20] In particular, the transition $^5D_0 \rightarrow {}^7F_0$ is comparably quite strong in **5-Eu** and **6-Eu** which could be interesting for coherent spectroscopy and quantum information applications in the future.[21] Steady-state emission spectra in the solid state (powders, 298 K, $\lambda_{exc}$ = 532 nm) yield similar spectra compared to the solution data (see Figure S18 in the Supporting Information).

The luminescence lifetimes for the europium cryptates were measured in $D_2O$ ($\tau_{D_2O}$) and $H_2O$ ($\tau_{H_2O}$) at ambient temperature (see Table 1). For both cryptates, the determined lifetimes in $D_2O$ ($\tau_{D_2O}$(**5-Eu**) = 1.33 ms; $\tau_{D_2O}$(**6-Eu**) = 1.00 ms) are roughly twice as high as the measured values in $H_2O$ ($\tau_{H_2O}$(**5-Eu**) = 0.71 ms; $\tau_{H_2O}$(**6-Eu**) = 0.57 ms) which is not surprising due to quenching high-energy O−H stretching vibration overtones in aqueous solution. The observed values for $\tau$ in $D_2O$ and $H_2O$ as well as the magnitude of the isotope effect in deuterated solvents are very comparable to the ones previously reported for *N*-oxide containing tris(bipyridine) europium cryptates (see Table 1).[5,22] Based on the measured lifetimes, the number of inner-sphere water molecules q were evaluated using the empirical formula introduced by Beeby et al.[23] For **5-Eu** and **6-Eu**, the estimation of q yielded values of 0.5 and 0.6 respectively. The apparent number of inner-sphere water molecules are low and quite different compared to the values obtained for cryptates **1-Eu** ($q$ = 1.2) and **2-Eu** ($q$ = 1.3).[5] The only difference between the previously reported bipyridine-based cryptates and the ones investigated here is the presence of 1,10-phenanthroline. The bulkier phenanthroline, compared to bipyridine, may have a positive impact on shielding the metal center from coordinating solvent molecules. It should, however, also be mentioned that the empirical formula commonly used has primarily been developed for europium complexes with aminocarboxylate ligands.[23] It has been observed in the past that equations of this type for complexes with other ligand classes such as cryptates do not work as well for the unambiguous determination of $q$ values.[24] For the reasons outlined, the obtained, noninteger $q$ values or **5-Eu** and **6-Eu**, should not be overinterpreted and do not permit conclusive statements on the inner-sphere compositions at the present time.

Our core interest in this work is to achieve a further reduction of the radiative lifetime $\tau_{rad}$ and to receive more knowledge of how $\tau_{rad}$ can be utilized for lanthanoid complexes with high luminescence efficiencies. In case of europium(III), the estimation of $\tau_{rad}$ is a lot easier than for other lanthanoid cations because of its emissive transition $^5D_0 \rightarrow {}^7F_1$ which is magnetic-dipole (MD) allowed. If this transition is taken as constant and independent of the ligand environment, the radiative lifetime can easily be determined experimentally by using eq 3, which relates the total integrated emission from the $^5D_0$ level ($I_{tot}$) to the integrated emission of the $^5D_0 \rightarrow {}^7F_1$ band ($I_{MD}$).[2b]

$$\frac{1}{\tau_{rad}} = A_{MD,0} \cdot n^3 \cdot \frac{I_{tot}}{I_{MD}} \quad (3)$$

Thus, the radiative lifetime can be estimated from the corrected emission spectrum, the spontaneous emission probability for the $^5D_0 \rightarrow {}^7F_1$ transition in vacuo $A_{MD,0}$ = 14.65 $s^{-1}$ (see ref 2b) and the refractive index n. In agreement with the initial hypothesis of our study, phenanthroline does indeed have a positive effect on the radiative lifetime: Compared to the tris(bipyridine) cryptates **1-Eu** with two pyridine-*N*-oxides ($\tau_{rad}$ = 5.3 ms) and **2-Eu** with four pyridine-*N*-oxides ($\tau_{rad}$ = 3.6 ms),[5] the radiative lifetime upon incorporation of phenanthroline moieties into the cryptand scaffolds decreases even further for **5-Eu** with two pyridine-*N*-oxides ($\tau_{rad}$ = 2.9 ms) and finally to the lowest value for **6-Eu** with four pyridine-*N*-oxides ($\tau_{rad}$ = 2.0 ms). For comparison, we also studied the emission spectrum in the solid state. With the assumption of $n$ = 1.5 (see ref 2c) and using eq 3, $\tau_{rad}$ can also be obtained. Qualitatively, also very short radiative lifetimes are observed (**5-Eu**: $\tau_{rad}$ = 1.6 ms/**6-Eu**: $\tau_{rad}$ = 1.8 ms). There is a clear trend from **1-Eu** to **6-Eu** in solution: Higher *N*-oxide- as well as phenanthroline-contents result in shorter radiative lifetimes $\tau_{rad}$ and therefore make the emission more competitive compared to nonradiative deactivation processes. Combining the two effects reduces $\tau_{rad}$ by an impressive 62% going from **1-Eu** to **6-Eu**.

Using the measured lifetimes $\tau_{obs}$ in $D_2O$ (see text above or Table 1) and the radiative lifetimes obtained above, the intrinsic quantum yields in $D_2O$ according to eq 2 amount to $Q_{Ln}^{Ln}$ = 46% for **5-Eu** and to $Q_{Ln}^{Ln}$ = 50% **6-Eu** (Table 1) which is a significant improvement compared to **1-Eu** ($Q_{Ln}^{Ln}$ = 30%) and **2-Eu** ($Q_{Ln}^{Ln}$ = 28%)[5] and illustrates the potential of the rigidly planar phenanthroline units in both new europium cryptates. Concomitantly, there is a second benefit of introducing phenanthroline into the cryptand scaffolds: As can be seen from Table 1, the negative impact of increasing the *N*-oxide content on the already low sensitization efficiencies $\eta_{sens}$ seen in tris(bipyridine)-based cryptates **1-Eu** ($\eta_{sens}$ = 25%) and **2-Eu** ($\eta_{sens}$ = 15%) is absent. Instead, the phenanthroline-based cryptates show a much higher sensitization efficiency $\eta_{sens}$ for **5-Eu** ($\eta_{sens}$ = 78%) and $\eta_{sens}$ does not drop with an increase in *N*-oxide content going to **6-Eu** ($\eta_{sens}$ = 83%). The absolute quantum yields $Q_{Eu}^{L}$ of the phenanthroline-containing cryptates


https://doi.org/10.1021/acs.inorgchem.5c05828
Inorg. Chem. XXXX, XXX, XXX−XXX

in $D_2O$ were measured against quinine sulfate as standard.[25] The quantum yields are very high (Table 1: $Q^L_{Eu}$ = 36% for **5-Eu**; $Q^L_{Eu}$ = 42% for **6-Eu**) and stay very good even in $H_2O$ solution (Table 1: $Q^L_{Eu}$ = 20% for both **5-Eu** and **6-Eu**). With cryptates of this type already being known to be suitable for biomedical applications,[26] this particular result bodes well for future applicability of the new europium luminophores. In fact, the obtained absolute quantum yield are among the highest values for europium luminophores in aqueous solution.[27] It is quite striking that a simple substitution of 1,10-phenanthroline for 2,2′-bipyridine is responsible for the up to 10-fold increase of absolute quantum yield (Table 1: e.g. absolute quantum yield increase in $D_2O$ from $Q^L_{Eu}$ = 4.2% for **2-Eu** to $Q^L_{Eu}$ = 40% for **6-Eu**). There are several photophysical benefits that synergistically combine when replacing phenanthroline units for some of the bipyridine moieties in these cryptates. Based on the results, we can confirm that phenanthroline substantially lowers the radiative lifetime $\tau_{rad}$ for $Eu^{3+}$ compared to the analogous cryptates featuring only bipyridine-based units which will prove a useful design principle for future improvements in luminophores of this type. The biggest impact, however, seems to be the considerable increase in $\eta_{sens}$ for the new europium cryptates with mixed phenanthroline/bipyridine antennae. It appears plausible that phenanthroline with its rigid, planar framework[9] allows less nonradiative deactivation before the energy transfer step from the ligand to the lanthanoid-centered excited states but this alone seems unlikely to account for the massive increase in sensitization efficiency. Especially the energies of critical states (e.g., potential CT states) which are involved within the sensitization pathway could be responsible for the observed enhancement. The lack of current understanding will certainly merit more in-depth investigations in the future.

**Ytterbium.** The ytterbium cryptates **6-Yb** and **[D$_8$]-6-Yb** expectedly show almost identical, normalized near-IR luminescence bands for the transition $^2F_{5/2} \rightarrow {}^2F_{7/2}$ ($\lambda_{em} \approx$ 1000 nm) in $CD_3OD$ after ligand excitation in the UV region (Figure 7).

Luminescence lifetime measurements (see Table 2) under the same conditions revealed the influence of the reduced multiphonon quenching in **[D$_8$]-6-Yb** ($\tau_{obs}$ = 34 $\mu$s) compared to **6-Yb** ($\tau_{obs}$ = 25 $\mu$s). This observation is also manifestly visible in the increase in absolute quantum yields (Table 2: $Q^L_{Yb}$ = 2.2% for **6-Yb**; $Q^L_{Yb}$ = 2.7% for **[D$_8$]-6-Yb**). These quantum efficiencies are very respectable compared to other, known ytterbium luminophores in the literature.[1,2] In order to get a more detailed picture of the photophysical parameters, the radiative lifetimes were also determined in $CD_3OD$.

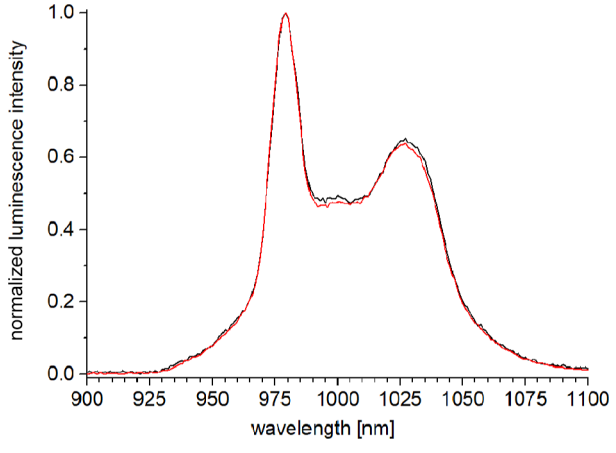


**Figure 7.** Normalized steady-state emission spectra ($CD_3OD$, $\lambda_{exc}$ = 305 nm, $c \approx$ 10 $\mu$M) for **6-Yb** (black) and **[D$_8$]-6-Yb** (red).

**Table 2. Luminescence Data for Ytterbium Cryptates 6-Yb and [D$_8$]-6-Yb in $CD_3OD$**

| compound | $\tau_{obs}$ [$\mu$s] | $\tau_{rad}$ [$\mu$s] | $Q^{Yb}_{Yb}$ [%] | $Q^L_{Yb}$ [%] | $\eta_{sens}$ [%] |
|---|---|---|---|---|---|
| **1-Yb**[4] | 12 | 1250 | - | - | 68 |
| **2-Yb**[4] | 26 | 658 | - | - | 46 |
| **6-Yb** | 25[a] | 612[b] | 4.1[c] | 2.2[d] | 52[e] |
| **[D$_8$]-6-Yb** | 34[a] | 612[b] | 5.5[c] | 2.7[d] | 49[e] |

[a]Luminescence lifetimes: $\lambda_{exc}$ = 305 nm, $\lambda_{em}$ = 979 nm ($^2F_{5/2} \rightarrow {}^2F_{7/2}$), estimated uncertainty ±10%. [b]Radiative lifetime calculated using the equation in the Supporting Information (see Section 5), estimated uncertainty ±20%. [c]Intrinsic quantum yield, estimated uncertainty ±30%. [d]Absolute quantum yield, measured using [Yb(TTA)$_3$phen] in toluene as standard (ref 28), estimated uncertainty ±20%. [e]Sensitization efficiency (see eq 1).

In contrast to $Eu^{3+}$, where the special properties of the MD transition $^5D_0 \rightarrow {}^7F_1$ could be used to conveniently calculate $\tau_{rad}$ from the emission spectrum directly[2b] (vide supra), in the case of $Yb^{3+}$ $\tau_{rad}$ for $^2F_{5/2} \rightarrow {}^2F_{7/2}$ was derived from the quantitative evaluation of the absorption band $^2F_{7/2} \rightarrow {}^2F_{5/2}$.[2b] The corresponding spectra for both isotopologues **6-Yb** and **[D$_8$]-6-Yb** are almost identical and show molar extinction coefficients $\varepsilon < 10\ M^{-1}\ cm^{-1}$ which are typical for the Laporte-forbidden but spin-allowed transition in question (Figure 8). A

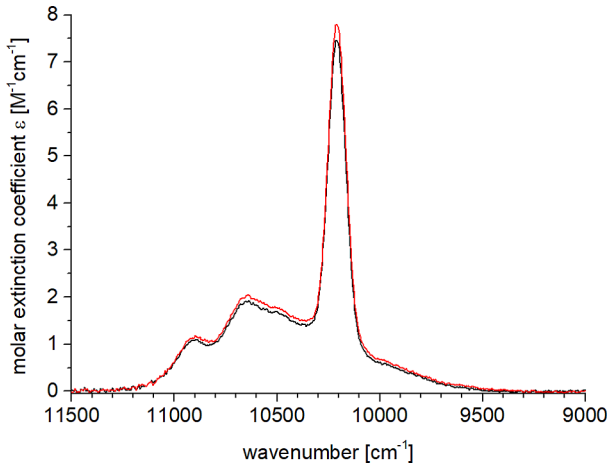


**Figure 8.** Absorption spectra ($CD_3OD$, $c \approx$ 3 mM) for the f–f transition $^2F_{7/2} \rightarrow {}^2F_{5/2}$ in **6-Yb** (black) and in **[D$_8$]-6-Yb** (red).

comparison of the f–f absorption and emission spectra for **6-Yb** shows the complementary fine-structure expected (Figure 9). Using a modified Einstein equation[2b] allowed the calculation of $\tau_{rad}$ (see the Supporting Information for details) for the new cryptates. **6-Yb** and **[D$_8$]-6-Yb** expectedly show the same $\tau_{rad}$ = 612 $\mu$s (Table 2). The obtained value is very short for molecular ytterbium complexes in solution.[1,2] The most relevant comparison can be made between **6-Yb** to the already very successul luminophore **2-Yb**[4] which in its perdeuterated form had an impressive quantum yield $Q^L_{Yb}$ = 12%.[4] Both systems seem very similar in a number of important photophysical parameters, e.g. $\tau_{obs}$ = 26 $\mu$s/$\tau_{rad}$ = 612 $\mu$s/$\eta_{sens}$ = 52% for **6-Yb** vs $\tau_{obs}$ = 25 $\mu$s/$\tau_{rad}$ = 658 $\mu$s and


https://doi.org/10.1021/acs.inorgchem.5c05828
Inorg. Chem. XXXX, XXX, XXX−XXX

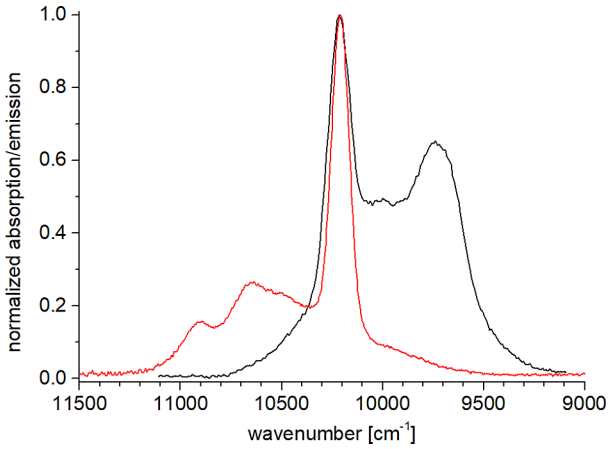


**Figure 9.** Comparison of the normalized absorption (red) and emission spectra (black, $\lambda_{exc}$ = 305 nm) for the f–f transition $^2F_{7/2} \leftrightarrow {}^2F_{5/2}$ of **6-Yb** in $CD_3OD$.

$\eta_{sens}$ = 46% for **2-Yb** (Table 2). In essence, the introduction of the phenanthroline motiv is not as effective for the improvement of ytterbium luminescence as it was shown for the corresponding europium cryptates **2-Eu** and **6-Eu** (vide supra), in part because **2-Yb** (unlike **2-Eu**) already showed high emission efficiency.

## CONCLUSION

In conclusion, we were able to integrate the rigidly planar 1,10-phenanthroline moiety into tris(biaryl)-*N*,*N*′-dioxide cryptand scaffolds. We have synthesized two europium(III) cryptates with different amounts of 1,10-phenanthroline- and 2,2′-bipyridine-*N*,*N*′-dioxide building blocks in their macrobicyclic frameworks, as well as two isotopologic, partially deuterated ytterbium(III) cryptates of one of the new phenanthroline cryptates. The Yb cryptates show very short radiative lifetimes $\tau_{rad}$, moderate sensitization efficiencies $\eta_{sens}$ and good absolute quantum yields $Q^L_{Yb}$ but they do not significantly outperform their all-bipyridine counterparts. In contrast, replacing 2,2′-bipyridine by 1,10-phenanthroline in the europium cryptates leads to a considerable reduction of $\tau_{rad}$ but also a remarkable improvement in $\eta_{sens}$ and $Q^L_{Eu}$. Absolute quantum yields of up to 42% in $D_2O$ and 20% in $H_2O$ for **6-Eu** show great promise for the large number of lanthanoid luminescence applications in aqueous media, for example biomolecule labeling or time-resolved fluorescence energy transfer.

## EXPERIMENTAL SECTION

### General Information

Unless stated otherwise, starting materials and reagents were purchased from commercial suppliers and used as received. Airsensitive reactions were carried out under an inert atmosphere of argon using Schlenk technique. All solvents used for synthesis and purification were of HPLC grade purity. $CH_3CN$ was dried using a MBraun SPS-800 solvent purification system. Deuterated solvents had deuterium contents >99.5%D. Lanthanoid salts with 99.99% purity (REO) were used for the preparation of europium and lutetium cryptates, for ytterbium the purity was 99.995% (REO). Column chromatography was performed using silica gel 60 (Merck, 40–63 μm), aluminum oxide 60 (Acros Organics, neutral, Brockmann I, 40–300 μm) or aluminum oxide 90 (Macherey-Nagel and Merck, neutral and basic, Brockmann I, 63–200 μm). Analytical thin layer chromatography (TLC) was done on silica gel 60 $F_{254}$ plates (Merck, coated on aluminum sheets) or aluminum oxide 60 $F_{254}$, neutral plates (Supelco, coated on aluminum sheets).

NMR spectra were recorded on Bruker Avance III HD 300 ($^1$H: 300 MHz), Bruker AVII+400 ($^1$H: 400 MHz), Bruker AVII+500 ($^1$H: 500 MHz), Bruker Avance III HDX 600 ($^1$H: 600 MHz) or Bruker Avance III HDX 700 ($^1$H: 700 MHz) spectrometers. All chemical shifts ($\delta$) are reported in parts per million (ppm) relative to tetramethyl silane ($^1$H, $^{13}$C) and trichlorofluoromethane ($^{19}$F). The solvents' residual signals were used as internal reference ($^1$H, $^{13}$C). Observed signal multiplicities and broad lines are specified as s (singlet), d (doublet), t (triplet), q (quartet), m (multiplet), br (broad).

ESI mass spectra were measured by the Analytics Department of the University of Tübingen using Bruker amaZon SL and Bruker maXis.

Elemental analysis was performed by the Central Analytical Facility of the Chemistry Department of the University of Tübingen with a VarioMicro V1.9.2. analysis system.

Reversed-phase(RP)-HPLC was performed using Lichrospher RP-18e columns (Merck, semipreparative: 250 mm × 10 mm, 10 μm particle size; analytical: 125 mm × 4 mm, 5 μm particle size) on a Knauer AZURA P6.1L system. For more details see the Supporting Information.

### Synthesis

**Diamine 7.** A solution of hexamethylenetetramine (575 mg, 4.1 mmol, 5.0 equivs) in $CHCl_3$ (40 mL, HPLC grade) was refluxed and 2,9-bis(bromomethyl)-1,10-phenanthroline (**8**)[12] (300 mg, 0.82 mmol, 1.0 equiv) in $CHCl_3$ (60 mL, HPLC grade) was added dropwise. A colorless precipitate formed and the mixture was refluxed for additional 2 h. The mixture was allowed to cool and to stand for 16 h at room temperature. The precipitate was removed by filtration, washed with $CHCl_3$ (25 mL, HPLC grade) and dried in vacuo. Addition of a mixture of water (2.1 mL), ethanol (8.3 mL) and 48% HBr (2.5 mL) at 82 °C (bath temperature) yielded a bronze colored solution. The solution was allowed to cool down overnight and the bronze colored, crystalline platelets were filtered off, washed with cold ethanol and dried (89 mg, 0.18 mmol, 22%).

$^1$H NMR (400 MHz, [$D_6$]-DMSO): $\delta$ 8.63 (d, $J$ = 8.3 Hz, 2H), 8.51 (s br, 6H), 8.09 (s, 2H), 7.90 (d, $J$ = 8.2 Hz, 2H), 4.58 (q, $J$ = 5.8 Hz, 4H) ppm. $^{13}$C NMR (63 MHz, DMSO-$d_6$): $\delta$ 153.4, 143.5, 137.7, 128.1, 126.7, 122.1, 43.1 ppm. MS (ESI, pos. mode): $m/z$ (%) = 239.2 (100, $[M + H]^+$). Elemental analysis: Anal. Calcd for $C_{14}H_{17}N_4Br_3$ ($M_r$ = 481.03): C, 34.96; H, 3.56; N, 11.65. Found: C, 34.69; H, 3.53; N, 11.30.

**Sodium Cryptate 5-Na.** A suspension of dibromide **8**[12] (30 mg, 82 μmol, 1.0 equiv), diamine **7** (40 mg, 83 μmol, 1.0 equiv), dibromide **9**[13] (31 mg, 82 μmol, 1.0 equiv) and $Na_2CO_3$ (119 mg, 1.12 mmol, 13.7 equivs) in $CH_3CN$ (300 mL, HPLC grade) was heated under reflux for 42 h. The heating bath was removed, the hot solution was filtered and all volatiles of the filtrate were removed in vacuo. The resulting residue was subjected to column chromatography ($SiO_2$, $CH_2Cl_2/CH_3OH$, gradient 9:1 → 7:1) yielding the title compound as a colorless solid (15 mg, 21 μmol, 26%).

$^1$H NMR (400 MHz, $CD_3OD$): $\delta$ 8.41 (d, $J$ = 8.2 Hz, 2H), 8.38 (d, $J$ = 8.2 Hz, 2H), 7.93 (dd, $J$ = 7.9, 2.0 Hz, 2H), 7.88 (dd, $J$ = 10.3, 8.8 Hz, 4H), 7.83 (dd, $J$ = 7.8, 2.0 Hz, 2H), 7.73 (d, $J$ = 5.2 Hz, 2H), 7.71 (d, $J$ = 5.1 Hz, 2H), 7.65 (t, $J$ = 7.8 Hz, 2H), 4.56 (d, $J$ = 11.7 Hz, 2H), 4.40 (d, $J$ = 14.8 Hz, 2H), 4.09 (d, $J$ = 14.7 Hz, 2H), 3.98 (d, $J$ = 14.8 Hz, 2H), 3.87 (d, $J$ = 15.0 Hz, 2H), 3.58 (d, $J$ = 11.6 Hz, 2H) ppm. $^{13}$C NMR (100 MHz, $CD_3OD$): $\delta$ 160.2, 159.4, 150.5, 147.3, 147.0, 146.5, 138.7, 138.7, 131.4, 129.8, 129.8, 128.6, 128.5, 127.4, 127.4, 124.8, 124.7, 63.0, 61.5, 55.7 ppm. MS (ESI pos. mode): $m/z$ (%) = 677.5 (100, [M]+). $R_f$ = 0.5 ($SiO_2$, $CH_2Cl_2$/MeOH 4:1, UV detection).

**Sodium Cryptate 6-Na.** A suspension of diamine **7** (60 mg, 125 μmol, 1.0 equiv), dibromide **9**[13] (94 mg, 250 μmol, 2.0 equivs) and $Na_2CO_3$ (133 mg, 1.25 mmol, 10.0 equivs) in $CH_3CN$ (250 mL, HPLC grade) was heated under reflux for 40 h. The heating bath was removed, the hot solution was filtered and all volatiles of the filtrate


https://doi.org/10.1021/acs.inorgchem.5c05828
Inorg. Chem. XXXX, XXX, XXX–XXX

were removed in vacuo. Column chromatography (neutral alumina 90, activity I, $CH_2Cl_2/CH_3OH$ 20:1) yielded the cryptate as yellowish, iridescent platelets (60 mg, 78 μmol, 63%).

Single crystal suitable for X-ray diffraction were grown from methanolic solution of **6-Na** by slow vapor diffusion of $Et_2O$.

$^1$H NMR (400 MHz, $CD_3OD$): δ 8.39 (d, *J* = 8.4 Hz, 2H), 7.91 (dd, *J* = 7.7, 2.1 Hz, 2H), 7.87 (s, 2H), 7.80 (dd, *J* = 8.0, 1.9 Hz, 2H), 7.75−7.64 (m, 8H), 7.49 (t, *J* = 7.9 Hz, 2H), 4.59 (d, *J* = 12.0 Hz, 2H), 4.42 (d, *J* = 11.6 Hz, 2H), 4.14 (d, *J* = 15.2 Hz, 2H), 4.00 (d, *J* = 15.6 Hz, 2H), 3.53 (d, *J* = 12.0 Hz, 2H), 3.53 (d, *J* = 12.0 Hz, 2H) ppm. $^{13}$C NMR (100 MHz, $CD_3OD$): δ 159.6, 149.6, 149.5, 147.3, 146.9, 146.2, 138.9, 131.4, 130.7, 130.3, 129.2, 128.9, 127.8, 127.7, 126.9, 124.9, 63.1, 56.6, 55.8 ppm. MS (ESI, pos. mode): *m*/*z* (%) = 685.3 (100, $[M]^+$). $R_f$ = 0.2 (neutral $Al_2O_3$, $CH_2Cl_2/CH_3OH$ 20:1, UV detection).

**Sodium Cryptate [D$_8$]-6-Na.** A suspension of diamine **7** (50 mg, 0.10 mmol, 1.0 equiv), partially deuterated dibromide [**D$_4$**]-**9**[14] (79 mg, 0.21 mmol, 2.1 equivs) and $Na_2CO_3$ (111 mg, 1.0 mmol, 10.0 equivs) in $CH_3CN$ (250 mL, HPLC grade) was heated under reflux for 46 h. The heating bath was removed, the hot solution was filtered and all volatiles of the filtrate were removed in vacuo. Column chromatography (neutral alumina 90, activity I, gradient $CH_2Cl_2/CH_3OH$ 50:1 to 20:1) yielded the cryptate as yellowish, iridescent platelets (50 mg, 71 μmol, 71%, 98%D from ESI-MS).

$^1$H NMR (400 MHz, $CD_3OD$): δ 8.38 (d, *J* = 8.3 Hz, 2H), 7.91 (dd, *J* = 7.7, 2.1 Hz, 2H), 7.86 (s, 2H), 7.80 (dd, *J* = 7.8, 2.0 Hz, 2H), 7.75−7.64 (m, 8H), 7.49 (t, *J* = 7.9 Hz, 2H), 4.14 (d, *J* = 15.2 Hz, 2H), 4.00 (d, *J* = 15.4 Hz, 2H) ppm. MS (ESI, pos. mode): *m*/*z* (%) = 693.3 (100, $[M]^+$). $R_f$ = 0.09 (neutral $Al_2O_3$, $CH_2Cl_2/CH_3OH$ 50:1, UV detection).

**Europium Cryptate 5-Eu.** Sodium cryptate **5-Na** (12 mg, 16 μmol, 1.0 equiv) and $EuCl_3{\cdot}6H_2O$ (13 mg, 35 μmol, 2.2 equivs) were suspended in $CH_3CN$ (15 mL, HPLC grade). After stirring the mixture, a colorless precipitate appeared immediately. The suspension was heated under reflux for 45 h, cooled and filtered through a membrane filter (nylon, 0.45 μm pore size). The colorless precipitate was washed with $CH_3CN$ and dried in vacuo. The crude product was dissolved in a minimum of water, filtered through a membrane filter (nylon, 0.45 μm pore size) and the filtrate was subjected to preparative reversed-phase HPLC (see the Supporting Information for details). Fractions containing pure lanthanoid complexes were combined (retention time $t_r$ = 21.5 min) and evaporated to dryness at room temperature to yield **5-Eu** as a colorless solid (11 mg, 9.6 μmol, 60%).

$^1$H NMR (400 MHz, $CD_3OD$): δ 27.12 (d, *J* = 15.68 Hz, 2H), 26.79 (d, *J* = 12.72 Hz, 2H), 14.88 (d, *J* = 8.48 Hz, 2H), 13.03 (d, *J* = 15.26 Hz, 2H), 11.28 (d, *J* = 8.48 Hz, 2H), 9.45−9.43 (m, 2H), 9.03 (t, *J* = 7.84 Hz, 2H), 7.01 (d, *J* = 8.48 Hz, 2H), 6.93 (d br, *J* = 11.44 Hz, 2H), 5.67 (d, *J* = 7.63 Hz, 2H), 4.45 (d, *J* = 8.48 Hz, 2H), 4.13 (d, *J* = 8.05 Hz, 2H), 3.38 (d, *J* = 8.05 Hz, 2H), −7.44 (d, *J* = 12.72 Hz, 2H), −12.00 (d, *J* = 13.99 Hz, 2H) ppm. $^{19}$F{$^1$H} NMR (376 MHz, $CD_3OD$): δ −77.98 (s br) ppm. MS (ESI, pos. mode, addition of HCOOH): *m*/*z* (%) = 403.06 (5, $[M + e^-]^{2+}$), 426.05 (100, $[M + HCOO^-]^{2+}$).

**Europium Cryptate 6-Eu.** Sodium cryptate **6-Na** (30 mg, 39 μmol, 1.0 equiv) and $EuCl_3{\cdot}6H_2O$ (26 mg, 70 μmol, 1.8 equivs) were suspended in $CH_3CN$ (40 mL, HPLC grade). The slightly yellow suspension was heated under reflux for 46 h. The solvent was removed in vacuo and the crude product was dissolved in a minimum of water, filtered through a membrane filter (nylon, 0.45 μm pore size) and the filtrate was subjected to preparative reversed-phase HPLC (see the Supporting Information for details). Fractions containing pure lanthanoid complexes were combined (retention time $t_r$ = 16.9 min) and evaporated to dryness at room temperature to yield **6-Eu** as a colorless solid (11 mg, 9.5 μmol, 24%).

$^1$H NMR (400 MHz, $CD_3OD$): δ 17.20 (d, 2H), 16.14 (s br, 2H), 15.19 (d, 2H), 11.41 (d, 2H), 11.18 (t, 2H), 9.54 (s br, 2H), 6.83 (d, 2H), 6.73 (m, 2H), 6.24 (s br, 2H), 4.87 (s br, 4H), 3.47 (s br, 4H), −1.78 (s br, 2H), −5.97 (s br, 2H) ppm. $^{19}$F{$^1$H} NMR (376 MHz, $CD_3OD$): δ −76.98 (s) ppm. MS (ESI, pos. mode, addition of HCOOH): *m*/*z* (%) = 407.05 (5, $[M + e^-]^{2+}$), 430.04 (100, $[M + HCOO^-]^{2+}$), 452.04 (60), 464.01 (52).

**Ytterbium Cryptate 6-Yb.** Sodium cryptate **6-Na** (31 mg, 41 μmol, 1.0 equiv) and $YbCl_3{\cdot}6H_2O$ (28.5 mg, 73 μmol, 1.8 equivs) were suspended in $CH_3CN$ (60 mL, HPLC grade). The slightly yellow suspension was heated under reflux for 68 h. Additional $YbCl_3{\cdot}6H_2O$ (8.0 mg, 21 μmol, 0.5 equivs) was added and heating was continued under reflux for further 14 h. The solvent was removed in vacuo. The crude product was dissolved in a minimum of MeOH and layered with $Et_2O$. The precipitate was collected and subjected to preparative reversed-phase HPLC (see the Supporting Information for details). Fractions containing pure lanthanoid complexes were combined (retention time $t_r$ = 9.1 min) and evaporated to dryness at room temperature to yield **6-Yb** as a colorless solid (12.5 mg, 11 μmol, 27%).

$^1$H NMR (400 MHz, $CD_3OD$): δ 99.4, 82.4, 72.9, 44.2, 29.7, 14.8, −1.43, −2.76, −7.08, −10.5 ppm. $^{19}$F{$^1$H} NMR (376 MHz, $CD_3OD$): δ −76.86 (s) ppm. MS (ESI, pos. mode, addition of HCOOH): *m*/*z* (%) = 440.58 (100, $[M + HCOO^-]^{2+}$).

**Ytterbium Cryptate [D$_8$]-6-Yb.** Sodium cryptate [**D$_8$**]-**6-Na** (35 mg, 45 μmol, 1.0 equiv) and $YbCl_3{\cdot}6H_2O$ (31.9 mg, 81 μmol, 1.8 equivs) were suspended in $CH_3CN$ (60 mL, HPLC grade). The slightly yellow suspension was heated under reflux for 50 h. Additional $YbCl_3{\cdot}6H_2O$ (9.0 mg, 23 μmol, 0.5 equivs) was added and heating was continued under reflux for further 50 h. The solvent was removed in vacuo. The crude product was subjected to preparative reversed-phase HPLC (see the Supporting Information for details). Fractions containing pure lanthanoid complexes were combined (retention time $t_r$ = 8.8 min) and evaporated to dryness at room temperature to yield the title compound as a colorless solid (17.9 mg, 15 μmol, 33%).

$^1$H NMR (400 MHz, $CD_3OD$): δ 100.4, 82.0, 44.2, 14.8, −1.33, −2.76, −7.03, ppm. $^{19}$F{$^1$H} NMR (376 MHz, $CD_3OD$): δ −76.84 (s) ppm. MS (ESI, pos. mode, addition of HCOOH): *m*/*z* (%) = 444.60 (100, $[M + HCOO^-]^{2+}$).

**Lutetium Cryptate 5-Lu.** Sodium cryptate **5-Na** (5.0 mg, 7.0 μmol, 1.0 equiv) and $LuCl_3{\cdot}6H_2O$ (5.0 mg, 14 μmol, 2.0 equivs) were suspended in $CH_3CN$ (7 mL, HPLC grade). The mixture was heated under reflux for 45 h. The solvent was removed in vacuo and the crude product was dissolved in a minimum of water, filtered through a membrane filter (nylon, 0.45 μm pore size) and the filtrate was subjected to preparative reversed-phase HPLC (see the Supporting Information for details). Fractions containing pure lanthanoid complexes were combined (retention time $t_r$ = 16.7 min) and evaporated to dryness at room temperature to yield **5-Lu** as a colorless solid (5 mg, 4 μmol, 56%).

$^1$H NMR (400 MHz, $CD_3OD$): δ 8.83 (d, *J* = 8.35 Hz, 2H), 8.74 (d, *J* = 8.32 Hz, 2H), 8.38 (dd, *J* = 7.29, 2.34 Hz, 2H), 8.28 (dd, *J* = 7.88, 2.56 Hz, 2H), 8.26−8.23 (m, 2H), 8.15 (dd, *J* = 9.89, 8.89 Hz, 4H), 8.06 (d, *J* = 8.37 Hz, 2H), 7.99 (d, *J* = 8.30 Hz, 2H), 4.97 (d, *J* = 15.33 Hz, 2H), 4.69 (d, *J* = 12.92 Hz, 2H), 4.43 (d, *J* = 15.97 Hz, 2H), 4.35 (d, *J* = 15.46 Hz, 2H), 4.15 (d, *J* = 15.80 Hz, 2H), 4.06 (d, *J* = 12.93 Hz, 2H) ppm.

**Lutetium Cryptate 6-Lu.** Sodium cryptate **6-Na** (5 mg, 7 μmol, 1.0 equiv) and $LuCl_3{\cdot}6H_2O$ (5 mg, 14 μmol, 2.0 equivs) were suspended in $CH_3CN$ (7 mL, HPLC grade). The mixture was heated under reflux for 45 h. The solvent was removed in vacuo and the crude product was dissolved in a minimum of water, filtered through a membrane filter (nylon, 0.45 μm pore size) and the filtrate was subjected to preparative reversed-phase HPLC (see the Supporting Information for details). Fractions containing pure lanthanoid complexes were combined (retention times $t_r$ = 15.0 min) and evaporated to dryness at room temperature to yield the **6-Lu** as a colorless solid (2 mg, 1 μmol, 21%).

$^1$H NMR (400 MHz, $CD_3OD$): δ 8.67 (d, 2H), 8.16 (dd, *J* = 7.58, 2.40 Hz, 2H), 8.13 (dd, *J* = 7.82, 1.82 Hz, 2H), 8.08−8.05 (m, 4H), 8.03 (dd, *J* = 7.85, 2.41 Hz, 2H), 8.00−7.92 (m, 6H), 4.65 (d, *J* = 12.67 Hz, 2H), 4.38 (d, *J* = 12.17 Hz, 2H), 4.33 (d, *J* = 16.36 Hz, 2H), 4.26 (d, *J* = 16.25 Hz, 2H), 3.89 (d, *J* = 12.10 Hz, 2H), 3.84 (d, *J* = 12.75 Hz, 2H) ppm.


https://doi.org/10.1021/acs.inorgchem.5c05828
Inorg. Chem. XXXX, XXX, XXX−XXX

### Photophysical Measurements

UV/vis spectra were measured on a Jasco V-770 spectrophotometer using quartz cuvettes (Suprasil, 1.0 cm path length) at room temperature.

A Horiba Fluorolog-3 spectrofluorometer equipped with a 450 W xenon lamp was used for steady-state measurements. Emission was detected in 90° geometry by a Hamamatsu R2658P PMT detector (200 nm < $\lambda_{em}$ < 1010 nm) in the visible region or by a Hamamatsu H10330−75 PMT detector (950 nm < $\lambda_{em}$ < 1700 nm) in the near-IR. Spectral selection in the excitation path was accomplished by a DFX monochromator (double gratings: 1200 grooves/mm, 330 nm blaze) and in the emission paths in the visible/near-IR spectral region ($\lambda_{em}$ < 1010 nm) by a spectrograph iHR550 (single gratings: either 1200 grooves/mm, 500 nm blaze or 950 grooves/mm, 900 nm blaze) and in the near-IR spectral region ($\lambda_{em}$ > 950 nm) by a spectrograph iHR320 (single grating: 600 grooves/mm, 1000 nm blaze). Spectral correction of the emission spectra was performed with a correction curve implemented by the instrument manufacturer. Absolute quantum yields $Q^L_{Ln}$ were determined in repeated experiments by the optically dilute method using the following eq 4

$$Q^L_{Ln} = \Phi_r \cdot (Grad_x/Grad_r) \cdot (n_x^2/n_r^2) \quad (4)$$

where $n$ is the refractive index ($H_2O$ = 1.334; $D_2O$ = 1.328; toluene: $n$ = 1.496; $CD_3OD$: $n$ = 1.326) and Grad is the linearly fitted slope from the plot of the integrated luminescence intensity versus the absorbance at the excitation wavelength. The subscripts x and r refer to the sample and reference, respectively. Quinine sulfate in 0.1 M sulfuric acid was used as reference for Eu emission with a fluorescence quantum yield of $\Phi_r$ = 54.6%.[25] For near-IR luminescence, [Yb(TTA)$_3$phen] in toluene was used with a quantum yield of $\Phi_r$ = 1.1%.[28]

The luminescence decay kinetics were determined at 298 K with a 70 W pulsed xenon flash lamp (pulse width ca. 2 $\mu$s fwhm). The analysis of the luminescence decay kinetics (deconvolution, statistical parameters, etc.) was performed using the software package DAS from Horiba.

Low temperature steady state emission spectra were recorded in a glassy matrix of $CH_3OH$/EtOH (1:1, v/v) in standard NMR tubes at 77 K (liquid nitrogen) using a low-temperature optical dewar.

Steady-state emission spectra of powder samples of **5-Eu** and **6-Eu** were measured at room temperature and an excitation wavelength of 532 nm (Cobolt Samba 0532−04−01−0100−500) using an Andor Shamrock 500i spectrograph (150 grooves/mm, 800 nm blaze), equipped with an Andor iVac 316B LDC-DD CCD sensor.

## ■ ASSOCIATED CONTENT

### Supporting Information

The Supporting Information is available free of charge at https://pubs.acs.org/doi/10.1021/acs.inorgchem.5c05828.

$^1$H NMR spectra, HPLC traces for the lanthanoid complexes, extended photophysical data, crystallographic details for **6-Na**, details for the calculation of $\tau_{rad}$ in **6-Yb** and [**D$_8$**]-**6-Yb** (PDF)

### Accession Codes

Accession Codes CCDC 2184715 contain the supplementary crystallographic data for this paper. These data can be obtained free of charge via www.ccdc.cam.ac.uk/data_request/cif, or by emailing data_request@ccdc.cam.ac.uk, or by contacting The Cambridge Crystallographic Data Centre, 12 Union Road, Cambridge CB2 1EZ, UK; fax: +44 1223 336033.

## ■ AUTHOR INFORMATION


### Corresponding Author

**Michael Seitz** − *Institute of Inorganic Chemistry, University of Tübingen, 72076 Tübingen, Germany*; orcid.org/0000-0002-9313-2779; Email: michael.seitz@uni-tuebingen.de

### Authors

**Tobias Haas** − *Institute of Inorganic Chemistry, University of Tübingen, 72076 Tübingen, Germany*

**Timo Neumann** − *Institute of Inorganic Chemistry, University of Tübingen, 72076 Tübingen, Germany*

**Nicholas Jobbitt** − *Institute of Physics (PHI), Karlsruhe Institute of Technology, 76131 Karlsruhe, Germany*

**Xiaoyu Yang** − *Institute of Physics (PHI), Karlsruhe Institute of Technology, 76131 Karlsruhe, Germany*

**Hartmut Schubert** − *Institute of Inorganic Chemistry, University of Tübingen, 72076 Tübingen, Germany*

**David Hunger** − *Institute of Physics (PHI) and Institute for Quantum Materials and Technologies (IQMT), Karlsruhe Institute of Technology, 76131 Karlsruhe, Germany*; orcid.org/0000-0001-6156-6145

Complete contact information is available at: https://pubs.acs.org/10.1021/acs.inorgchem.5c05828


### Notes

The authors declare no competing financial interest.

## ■ ACKNOWLEDGMENTS

D.H. and M.S. gratefully acknowledge financial support from the German Research Foundation (DFG) through the Collaborative Research Center "4f for Future" (CRC 1573, project number 471424360), projects C2 and C3. This work was also support by the Karlsruhe School of Optics and Photonics (KSOP) at the Karlsruhe Institute of Technology (KIT).

## ■ REFERENCES

(1) Selected reviews: (a) *Lanthanide Luminescence (Springer Series on Fluorescence 7)*; Hänninen, P., Härma, H., Eds.; Springer: Berlin, 2011. (b) Alexander, C.; Guo, Z.; Glover, P. B.; Faulkner, S.; Pikramenou, Z. Luminescent Lanthanides in Biorelated Applications: From Molecules to Nanoparticles and Diagnostic Probes to Therapeutics. *Chem. Rev.* **2025**, *125*, 2269. (c) Tessitore, G.; Mandl, G. A.; Maurizio, S. L.; Kaur, M.; Capobianco, J. A. The role of lanthanide luminescence in advancing technology. *RSC Adv.* **2023**, *13*, 17787.

(2) (a) Bünzli, J.-C. G.; Eliseeva, S. V. Photophysics of Lanthanoid Coordination Compounds. In *Comprehensive Inorganic Chemistry II*; Reedijk, J., Poeppelmeier, K., Eds.; Elsevier, 2013; pp 339−398. (b) Werts, M. H. V.; Jukes, R. T. F.; Verhoeven, J. W. The emission spectrum and the radiative lifetime of $Eu^{3+}$ in luminescent lanthanide complexes. *Phys. Chem. Chem. Phys.* **2002**, *4*, 1542. (c) Bünzli, J.-C. G.; Chauvin, A.-S.; Kim, H. K.; Deiters, E.; Eliseeva, S. V. Lanthanide luminescence efficiency in eight- and nine-coordinate complexes: Role of the radiative lifetime. *Coord. Chem. Rev.* **2010**, *254*, 2623.

(3) Eliseeva, S. V.; Pleshkov, D. N.; Lyssenko, K. A.; Lepnev, L. S.; Bünzli, J.-C. G.; Kuzmina, N. P. Deciphering Three Beneficial Effects of 2,2'-Bipyridine-N,N'-Dioxide on the Luminescence Sensitization of Lanthanide(III) Hexafluoroacetylacetonate Ternary Complexes. *Inorg. Chem.* **2011**, *50*, 5137.

(4) Doffek, C.; Seitz, M. The Radiative Lifetime in Near-IR-Luminescent Ytterbium Cryptates: The Key to Extremely High Quantum Yields. *Angew. Chem., Int. Ed.* **2015**, *54*, 9719.

(5) Trautnitz, M. F. K.; Doffek, C.; Seitz, M. Radiative Lifetime, Non-Radiative Relaxation, and Sensitization Efficiency in Lumines-



https://doi.org/10.1021/acs.inorgchem.5c05828
Inorg. Chem. XXXX, XXX, XXX−XXX

cent Europium and Neodymium Cryptates − The Roles of 2,2'-Bipyridine-N,N'-dioxide and Deuteration. *ChemPhysChem* **2019**, *20*, 2179.
(6) Selected recent examples: (a) Kovacs, D.; Borbas, K. E. The role of photoinduced electron transfer in the quenching of sensitized europium emission. *Coord. Chem. Rev.* **2018**, *364*, 1. (b) Nonat, A.; Esteban-Gómez, D.; Valencia, L.; Pérez-Lourido, P.; Barriada, J. L.; Charbonnière, L. C.; Platas-Iglesias, C. The role of ligand to metal charge-transfer states on the luminescence of Europium complexes with 18-membered macrocyclic ligands. *Dalton Trans.* **2019**, *48*, 4035. (c) Kovacs, D.; Kocsi, D.; Wells, J. A. L.; Kiraev, S. R.; Borbas, K. E. Electron transfer pathways in photoexcited lanthanide(III) complexes of picolinate ligands. *Dalton Trans.* **2021**, *50*, 4244.
(7) Zhang, J.; Chen, B.; Luo, X.; Dua, K. Eu(III) Complex-Doped PMMA Having Fast Radiation Rate and High Emission Quantum Efficiency. *Polym. Sci., Ser. B* **2013**, *55*, 158.
(8) Georgieva, I.; Trendafilova, N.; Zahariev, T.; Danchova, N.; Gutzov, S. Theoretical insight in highly luminescent properties of Eu(III) complex with phenanthroline. *J. Lumin.* **2018**, *202*, 192.
(9) Accorsi, G.; Listorti, A.; Yoosaf, K.; Armaroli, N. 1,10-Phenanthrolines: versatile building blocks for luminescent molecules, materials and metal complexes. *Chem. Soc. Rev.* **2009**, *38*, 1690.
(10) Kreidt, E.; Kruck, C.; Seitz, M. Nonradiative Deactivation of Lanthanoid Luminescence by Multiphonon Relaxation in Molecular Complexes. In *Handbook on the Physics and Chemistry of Rare Earths*; Bünzli, J.-C. G., Pecharsky, V. K., Eds.; Elsevier: Amsterdam, 2018; Vol. *53*, pp 35−79.
(11) Wang, Z.; Reibenspies, J.; Motekaitis, R. J.; Martell, A. E. Analogous procedure for 2,2-bipyridine Unusual Stabilities of 6,6'-Bis(aminomethyl)-2,2'-bipyridyl Chelates of Transition-metal Ions and Crystal Structures of the Ligand and its Copper(II) and Nickel(II) Complexes. *J. Chem. Soc., Dalton Trans.* **1995**, 1511−1518.
(12) Chandler, C. J.; Deady, L. W.; Reiss, J. A. Synthesis of some 2,9-Disubstituted-1,10-phenanthrolines. *J. Heterocycl. Chem.* **1981**, *18*, 599.
(13) Lehn, J.-M.; Roth, C. O. Synthesis and Properties of Sodium and Europium(III) Cryptates Incorporating the 2,2' Bipyridine 1,1'-Dioxide and 3,3′-Biisoquinoline 2,2'-Dioxide Units. *Helv. Chim. Acta* **1991**, *74*, 572.
(14) Doffek, C.; Alzakhem, N.; Bischof, C.; Wahsner, J.; Güden-Silber, T.; Lügger, J.; Platas-Iglesias, C.; Seitz, M. Understanding the Quenching Effects of Aromatic C-H- and C-D-Oscillators in Near-IR Lanthanoid Luminescence. *J. Am. Chem. Soc.* **2012**, *134*, 16413.
(15) (a) Rodriguez-Ubis, J.-C.; Alpha, B.; Plancherel, D.; Lehn, J.-M. Photoactive cryptands Synthesis of the sodium cryptates of macrobicyclic ligands containing bipyridine and phenanthroline groups. *Helv. Chim. Acta* **1984**, *67*, 2264. (b) Caron, A.; Guilhelm, J.; Riche, C.; Pascard, C.; Alpha, B.; Lehn, J.-M.; Rodriguez-Ubis, J. Photoactive cryptands Crystal structure of the sodium cryptate of the tris-(phenanthroline) macrobicyclic ligand. *Helv. Chim. Acta* **1985**, *68*, 1577−1582.
(16) Trautnitz, M. F. K.; Haas, T.; Schubert, H.; Seitz, M. Unexpected Discovery of Calcium Cryptates with Exceptional Stability. *Chem. Commun.* **2020**, *56*, 9874.
(17) Farrugia, L. J. Ortep-3 for Windows ORTEP-3 for Windows - a version of ORTEP-III with a Graphical User Interface (GUI). *J. Appl. Crystallogr.* **1997**, *30*, 565.
(18) Value for Eu(EtSO4)3 · 9 H2O in 0.2 M aqueous HClO4 Carnall, W. T.; Fields, P. R.; Rajnak, K. Electronic Energy Levels Of the Trivalent Lanthanide Aquo Ions. IV. $Eu^{3+}$. *J. Chem. Phys.* **1968**, *49*, 4450.
(19) Carnall, W. T.; Goodman, G. L.; Rajnak, K.; Rana, R. S. A systematic analysis of the spectra of the lanthanides doped into single crystal $LaF_3$. *J. Chem. Phys.* **1989**, *90*, 3443−3457.
(20) Binnemans, K. Interpretation of europium(III) spectra. *Coord. Chem. Rev.* **2015**, *295*, 1.
(21) Kuppusamy, S. K.; Hunger, D.; Ruben, M.; Goldner, P.; Serrano, D. Spin-bearing molecules as optically addressable platforms for quantum technologies. *Nanophotonics* **2024**, *13*, 4357.
(22) Prodi, L.; Maestri, M.; Balzani, V.; Lehn, J.-M.; Roth, C. Luminescence properties of cryptate europium(III) complexes incorporating heterocyclic N-oxide groups. *Chem. Phys. Lett.* **1991**, *180*, 45.
(23) Beeby, A.; Clarkson, I. M.; Dickins, R. S.; Faulkner, S.; Parker, D.; Royle, L.; de Sousa, A. S.; Williams, J. A. G.; Woods, M. Non-radiative deactivation of the excited states of europium, terbium and ytterbium complexes by proximate energy-matched OH, NH and CH oscillators: an improved luminescence method for establishing solution hydration states. *J. Chem. Soc., Perkin Trans. 2* **1999**, 493.
(24) Faulkner, S.; Beeby, A.; Carrie, M.-C.; Dadabhoy, A.; Kenwright, A. M.; Sammes, P. G. Time-resolved near-IR luminescence from ytterbium and neodymium complexes of the Lehn cryptand. *Inorg. Chem. Commun.* **2001**, *4*, 187.
(25) Melhuish, W. H. Quantum efficiencies of fluorescence of organic substances: Effect of solvent and concentration of the fluorescent solute. *J. Phys. Chem.* **1961**, *65*, 229.
(26) Zwier, J. M.; Bazin, H.; Lamarque, L.; Mathis, G. Luminescent Lanthanide Cryptates: from the Bench to the Bedside. *Inorg. Chem.* **2014**, *53*, 1854.
(27) Selected examples: (a) Delbianco, M.; Sadovnikova, V.; Bourrier, E.; Mathis, G.; Lamarque, L.; Zwier, J. M.; Parker, D. Bright, Highly Water-Soluble Triazacyclononane Europium Complexes To Detect Ligand Binding with Time-Resolved FRET Microscopy. *Angew. Chem., Int. Ed.* **2014**, *53*, 10718. (b) Abad-Galán, L.; Cieslik, P.; Comba, P.; Gast, M.; Maury, O.; Neupert, L.; Roux, A.; Wadepohl, H. Excited State Properties of Lanthanide(III) Complexes witha Nonadentate Bispidine Ligand. *Chem.—Eur. J.* **2021**, *27*, 10303. (c) Leygue, N.; Picard, C.; Faure, P.; Bourrier, E.; Lamarque, L.; Zwier, J. M.; Galaup, C. Design of novel tripyridinophane-based Eu(III) complexes as efficient luminescent labels for bioassay applications. *Org. Biomol. Chem.* **2021**, *20*, 182.
(28) Meshkova, S. B.; Topilova, Z. M.; Bolshoy, Z. M.; Beltyukova, S. V.; Tsvirko, M. P.; Venchikov, V. Y. Quantum Efficiency of the Luminescence of Ytterbium(III) β-Diketonates. *Acta Phys. Polym., A* **1999**, *95*, 983.




https://doi.org/10.1021/acs.inorgchem.5c05828
*Inorg. Chem.* XXXX, XXX, XXX−XXX